Particle tracking at cryogenic temperatures: the Fast Annihilation Cryogenic Tracking (FACT) detector for the AEgIS antimatter gravity experiment

2015 JINST 10 C02023

(http://iopscience.iop.org/1748-0221/10/02/C02023)

PUBLISHED BY IOP PUBLISHING FOR SISSA MEDIALAB

RECEIVED: *September 30, 2014*
ACCEPTED: *November 27, 2014*
PUBLISHED: *February 13, 2015*

10th INTERNATIONAL CONFERENCE ON POSITION SENSITIVE DETECTORS
7–12 SEPTEMBER 2014,
UNIVERSITY OF SURREY, GUILDFORD, SURREY, U.K.

Particle tracking at cryogenic temperatures: the Fast Annihilation Cryogenic Tracking (FACT) detector for the AEgIS antimatter gravity experiment

The AEgIS collaboration

J. Storey,[c,1] **S. Aghion,**[a,b] **C. Amsler,**[c] **A. Ariga,**[c] **T. Ariga,**[c] **A. Belov,**[d] **G. Bonomi,**[e,f] **P. Braunig,**[g] **J. Bremer,**[h] **R. Brusa,**[i,j] **L. Cabaret,**[k] **M. Caccia,**[l,b] **R. Caravita,**[m,n] **F. Castelli,**[o,b] **G. Cerchiari,**[q] **K. Chlouba,**[r] **S. Cialdi,**[o,b] **D. Comparat,**[k] **G. Consolati,**[a,b] **H. Derking,**[h] **L. Di Noto,**[m,n] **M. Doser,**[h] **A. Dudarev,**[h] **A. Ereditato,**[c] **R. Ferragut,**[a,b] **A. Fontana,**[f] **S. Gerber,**[h] **M. Giammarchi,**[b] **A. Gligorova,**[r] **S. Gninenko,**[d] **S. Haider,**[h] **S. Hogan,**[s] **H. Holmestad,**[t] **T. Huse,**[t] **E.J. Jordan,**[p] **J. Kawada,**[c] **A. Kellerbauer,**[p] **M. Kimura,**[c] **D. Krasnicky,**[m,n] **V. Lagomarsino,**[m,n] **S. Lehner,**[u] **A. Magnani,**[f,y] **C. Malbrunot,**[h] **S. Mariazzi,**[u] **V. Matveev,**[d] **Z. Mazzotta,**[o,b] **G. Nebbia,**[v] **P. Nedelec,**[w] **M. Oberthaler,**[g] **N. Pacifico,**[r] **L. Penasa,**[i,j] **V. Petracek,**[q] **C. Pistillo,**[c] **F. Prelz,**[b] **M. Prevedelli,**[x] **L. Ravelli,**[i,j] **C. Riccardi,**[y,f] **O.M. Røhne,**[t] **S. Rosenberger,**[h] **A. Rotondi,**[y,f] **H. Sandaker,**[r] **R. Santoro,**[l,b] **P. Scampoli,**[x] **M. Simon,**[u] **M. Spacek,**[q] **I.M. Strojek,**[q] **M. Subieta,**[f,g] **G. Testera,**[n] **R. Vaccarone,**[n] **E. Widmann,**[u] **P. Yzombard,**[k] **S. Zavatarelli**[n] **and J. Zmeskal**[u]

[a] *Politecnico of Milano, Piazza Leonardo da Vinci 32, 20133 Milano, Italy*
[b] *INFN Milano, via Celoria 16, 20133 Milano, Italy*
[c] *Laboratory for High Energy Physics, Albert Einstein Center for Fundamental Physics, University of Bern, 3012 Bern, Switzerland*
[d] *Institute for Nuclear Research of the Russiam Academy of Science, Moscow 117312, Russia*
[e] *Department of Mechanical and Industrial Engineering, University of Brescia, via Branze 38, 25123 Brescia, Italy*
[f] *INFN Pavia, via Bassi 6, 27100 Pavia, Italy*
[g] *Kirchhoff-Institute for Physics, Heidelberg University, Im Neuenheimer Feld 227, 69120 Heidelberg, Germany*
[h] *Physics Department, CERN, 1211 Geneva 23, Switzerland*

[1] Corresponding author.

doi:10.1088/1748-0221/10/02/C02023

[i]Department of Physics, University of Trento, via Sommarive 14, 38123 Trento, Italy
[j]TIFPA/INFN Trento, via Sommarive 14, 38123 Trento, Italy
[k]Laboratory Aimé Cotton, CNRS, University of Paris-Sud, ENS Cachan, Bãt. 505, 91405 Orsay, France
[l]Department of Science, University of Insubria, Via Valleggio 11, 22100 Como, Italy
[m]Department of Physics, University of Genova, via Dodecaneso 33, 16146 Genova, Italy
[n]INFN Genova, via Dodecaneso 33, 16146 Genova, Italy
[o]Department of Physics, University of Milano, via Celoria 16, 20133 Milano, Italy
[p]Max Planck Institute for Nuclear Physics, Saupfercheckweg 1, 69117 Heidelberg, Germany
[q]Czech Technical University, Prague, Brehová 7, 11519 Prague 1, Czech Republic
[r]Institute of Physics and Technology, University of Bergen, Allégaten 55, 5007 Bergen, Norway
[s]University College London, London, U.K.
[t]Department of Physics, University of Oslo, Sem Sælandsvei 24, 0371 Oslo, Norway
[u]Stefan Meyer Institute for Subatomic Physics, Austrian Academy of Sciences, Boltzmanngasse 3, 1090 Vienna, Austria
[v]INFN Padova, via Marzolo 8, 35131 Padova, Italy
[w]Institute of Nuclear Physics, CNRS/IN2p3, University of Lyon 1, 69622 Villeurbanne, France
[x]University of Bologna, Viale Berti Pichat 6/2, 40126 Bologna, Italy
[y]Department of Physics, University of Pavia, via Bassi 6, 27100 Pavia, Italy

E-mail: james.storey@cern.ch

ABSTRACT: The AEgIS experiment is an interdisciplinary collaboration between atomic, plasma and particle physicists, with the scientific goal of performing the first precision measurement of the Earth's gravitational acceleration on antimatter. The principle of the experiment is as follows: cold antihydrogen atoms are synthesized in a Penning-Malmberg trap and are Stark accelerated towards a moiré deflectometer, the classical counterpart of an atom interferometer, and annihilate on a position sensitive detector. Crucial to the success of the experiment is an antihydrogen detector that will be used to demonstrate the production of antihydrogen and also to measure the temperature of the anti-atoms and the creation of a beam. The operating requirements for the detector are very challenging: it must operate at close to 4 K inside a 1 T solenoid magnetic field and identify the annihilation of the antihydrogen atoms that are produced during the 1 μs period of antihydrogen production. Our solution — called the FACT detector — is based on a novel multi-layer scintillating fiber tracker with SiPM readout and off the shelf FPGA based readout system. This talk will present the design of the FACT detector and detail the operation of the detector in the context of the AEgIS experiment.

KEYWORDS: Particle tracking detectors; Scintillators, scintillation and light emission processes (solid, gas and liquid scintillators)

2015 JINST 10 C02023

Contents

2015 JINST 10 C02023

1 The AEgIS experiment

The AEgIS experiment aims to measure the gravitational free-fall of the antihydrogen atom in order to test Einstein's principle of weak equivalence between inertial and gravitational mass with a system composed entirely of antiparticles [1, 2]. The aim is to measure the gravitational acceleration (gbar) on the antihydrogen atoms with an initial 1% accuracy by measuring the deflection and time of flight of the atoms as they traverse a moire deflectometer. This requires the production of a pulsed beam of antihydrogen atoms, the synthesis of which is a considerable challenge and the current focus of research. The scheme to produce the pulsed antihydrogen beam is illustrated in figure 1. Antiprotons from CERN's antiproton decelerator are loaded into a Penning-Malmberg trap and cooled to 100 mK. Positronium is produced in a nanoporous silicon target by implanting a bunch of 10^8 positrons. The longer lived ortho-positronium diffuses out of the target and is excited by lasers to Rydberg levels. The Rydberg positronium enters the Penning-Malmberg trap by means of a semi-transparent Penning trap electrode, where it then overlaps the cloud of antiprotons and forms Rydberg antihydrogen by means of a charge exchange reaction between the Rydberg positronium and cold antiprotons. Since the antihydrogen is neutral it is not confined in the Penning-Malmberg trap and will spread out isotropically. However, in order to use as much of the antihydrogen formed for the gravity measurement as possible, an electric field gradient is applied to accelerate the Rydberg antihydrogen atoms (which have a strong electric dipole moment) in the direction of the moire deflectometer. Further details of the AEgIS experiment can be found in references [3–6].

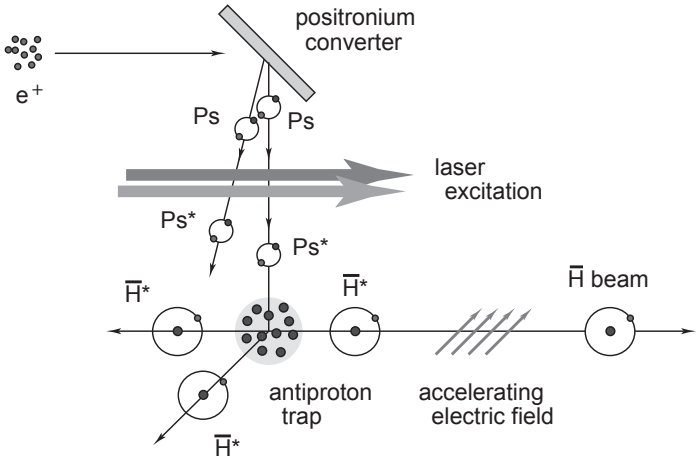

Figure 1. The AEgIS scheme to produce a pulsed antihydrogen beam.

2 Antihydrogen detection

2.1 Direct detection of antihydrogen production

Detection of antihydrogen production is a crucial requirement for the AEgIS experiment. In the absence of any time varying electric fields, the antihydrogen formed in the Penning-Malmberg trap will drift isotropically and typically annihilate on the inner surface of a trap electrode. The constituent antiproton annihilates into 2-3 150 MeV/c charged pions and the positron annihilates into two collinear 511 keV photons. The first direct detection of antihydrogen production was performed by the ATHENA collaboration who used the annihilation of the antiproton and positron to identify antihydrogen production [7]. The ATHENA antihydrogen detector consisted of a two layer silicon strip tracking detector and CsI crystals, which surrounded the Penning-Malmberg traps in which the antihydrogen was produced. The pions tracks were reconstructed with the silicon strip detector and extrapolated back to identify the antiproton annihilation vertex, while the CsI crystals were used to identify the 511 keV photons. For each reconstructed antiproton vertex an angle ($\theta_{\gamma\gamma}$) was calculated for two lines connecting the vertex and hit CsI crystals. The production of antihydrogen was identified by events for which cos($\theta_{\gamma\gamma}$)=-1. A similar technique was also used more recently by the ALPHA collaboration to detect the production and trapping of antihydrogen atoms. However, unlike the ATHENA detector, the ALPHA antihydrogen detector only identifies the location and time of the constituent antiproton annihilation and used the spatial distribution of these vertices to distinguish between antihydrogen and bare antiproton annihilations [8].

2.2 Antihydrogen detection requirements for AEgIS

The antihydrogen detector is required to measure the production of antihydrogen atoms, but also the temperature of the atoms produced and identify the formation of a beam. The operating environment is extremely challenging: the detector must operate at close to 4 K inside a cylindrical vacuum vessel which is co-axial to the Penning-Malmberg trap with an inner radius of 68 mm and an outer radius of 103 mm, inside a 1 T solenoid magnetic field and produce not more than 10 W of heat. Since antihydrogen is produced in a pulse the detector must be fast enough to identify each

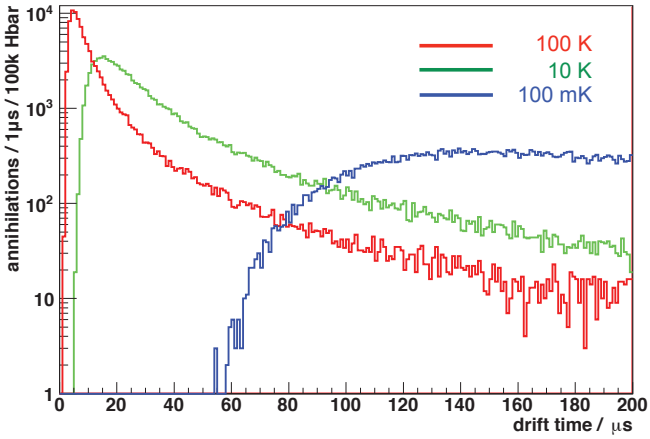

Figure 2. Drift time of antihydrogen atoms from production (t = 0 s) to the point of annihilation on the Penning-Malmberg trap wall, for antihydrogen synthesized with a mean temperature of 100 mK, 10 K and 100 K.

of the 100 or so antihydrogen atoms that are produced. The expected drift time of antihydrogen atoms from production to annihilation on the trap electrode wall is shown in figure 2 for different antihydrogen temperatures. For antihydrogen produced with a mean temperature of 10 K, 50 % of annihilations occur less than 500 ns after the previous annihilation.

3 The Fast Annihilation Cryogenic Tracking (FACT) detector

3.1 Detector design

In light of these requirements an antihydrogen detector has been developed for AEgIS based on scintillating plastic fiber and silicon photomultiplier technologies. An illustration of the Fast Annihilation Cryogenic Tracking (FACT) detector is shown in figure 3. Kuraray SCSF-78M multi-clad scintillating fibers of 1 mm diameter [9] are arranged in loops aligned orthogonally to the beam axis and operate at close to 4 K. There are two layers of scintillating fibers, each composed of two superimposed rows, at radial distances of 70 mm and 98 mm from the beam axis. Each layer consists of 400 scintillating fibers separated by 0.6 mm, with alternate fibers displaced radially by 0.8 mm in order to eliminate any gaps in the detector's solid angle. Each scintillating fiber is mechanically coupled to a clear fiber, which transports scintillation light to a Hamamatsu Multi-Pixel-Photon-Counters (MPPC) [10] located at room temperature approximately 2 m downstream of the detector. Readout and bias of the MPPCs is provided by electronics that is mounted outside of the vacuum via an electrical feedthrough. The design allows for reconstruction of the axial and radial position and time of each annihilation vertex, knowledge of which is sufficient to demonstrate antihydrogen production and beam formation. The antihydrogen temperature is measured by means of the time-of-flight and flight distance. From simulations an axial annihilation vertex resolution of $\sigma = 2.1$ mm is expected, which meets the AEgIS requirements.

3.2 Construction of the scintillating fiber tracker

Each of the two scintillating fiber layers are mounted on a 240 mm long cylindrical support structure made from 7075 aluminum. Each fiber on the bottom row of each layer is mechanically located

2015 JINST 10 C02023

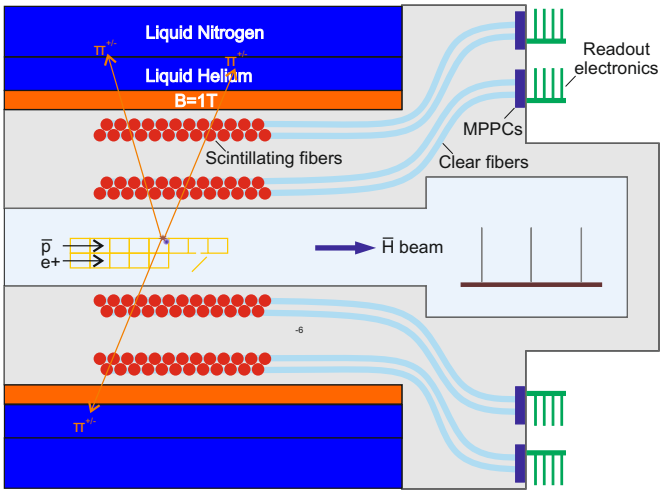

Figure 3. Conceptual design of the Fast Annihilation Cryogenic Tracking (FACT) detector for the identification of antihydrogen annihilations. Charged pions (orange lines) from the antihydrogen annihilation are reconstructed by the scintillating fiber tracker and extrapolated back to the antihydrogen formation region to identify the annihilation vertex.

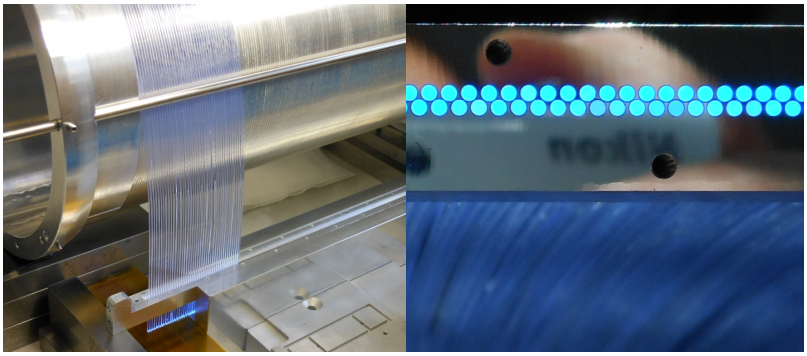

Figure 4. *Left*: mounting scintillating fibers into one part of the mechanical coupler prior to gluing. *Right*: scintillator side of the mechanical plate after diamond polishing.

in U shaped grooves that are machined into the support structure with a CNC milling machine to a precision of 10 μm. On each layer the top row of fibers are located in the gap between neighboring fibers on the bottom row. A key component of the design is the coupling between the scintillating and clear fibers, which requires a high transmission efficiency and reliability at low temperatures. The coupling between the fibers on each layer is mechanical and consists of a pair of 7075 aluminum alloy plates in which 1.05 mm holes are drilled to hold the fibers. The fibers are glued into the plate with a low viscosity epoxy (Stycast 2850-FT) and then polished with a diamond tool to a planarity of better than 10 μm. Guide pins along the length of the connector ensure the alignment of the scintillating and clear fibers. The production of the connector is shown in figure 4. After polishing the two scintillating fiber connectors are attached to the cylindrical support structures of each layer and the scintillating fibers are held in place by stainless steel rods that extend across the length of the support. Issues of thermal contraction are an important consideration

2015 JINST 10 C02023

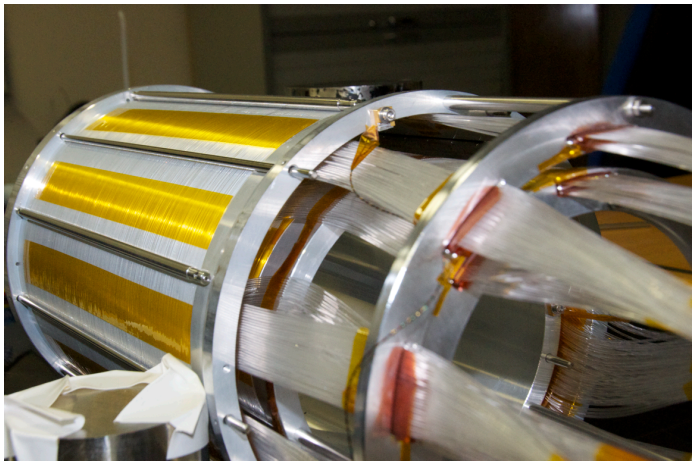

Figure 5. Fully acssembled scintillating fiber tracker. The clear fibers are arranged into groups of 25 fibers.

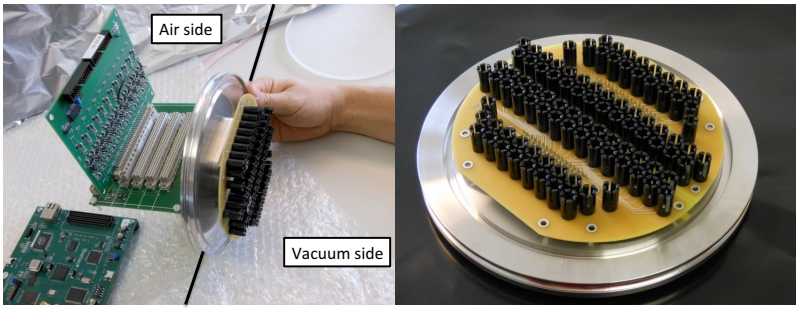

Figure 6. *Left*: vacuum and air side readout electronics. Two MPPC PCBs, each containing 48 MPPCs, are mounted on the vacuum side. The unamplified MPPC signal is routed through the feedthrough via a backplane PCB to one of four analogue boards. *Right*: MPPC PCBs mounted on vacuum feedthrough. A PT-1000 thermistor is mounted on each MPPC PCB and readout via a 15-pin DSub vacuum feedthrough.

in the design. To prevent strain on the fibers as they contract, the mechanical connector is the only point where the fibers are fixed to the support. The stainless steel rods constrain the radial distance of the fibers, but allow the fibers to slide around the support structure. The clear fibers are routed from the connector towards the readout electronics located 2 m downstream of the detector.

3.3 Readout electronics

The readout electronics is designed to detect the light from each scintillating fiber continuously for the 100 ms time window in which antihydrogen atoms are expected to annihilate. Each of the 800 scintillating fibers is connected, via a clear fiber, to a Hamamatsu 10362-11-100C MPPC with a photosensitive area of 1x1 mm^2. Each MPPC is placed in a two part plastic connector that is used to couple the MPPC to the clear fiber [11]. Groups of 48 MPPCs are soldered onto a PCB holder which connects to one of two 50-pin DSub vacuum feedthroughs that are mounted on a ISO-K 160 flange. An assembled MPPC PCB and vacuum feedthrough is shown in figure 6. Each clear fiber is glued into the other part of the 2-part plastic connector with epoxy (Stycast 2850-FT) and polished with a diamond tool. The fibers are each labeled with a system of colored glass beads that are attached to the clear fibers prior to gluing.

2015 JINST 10 C02023

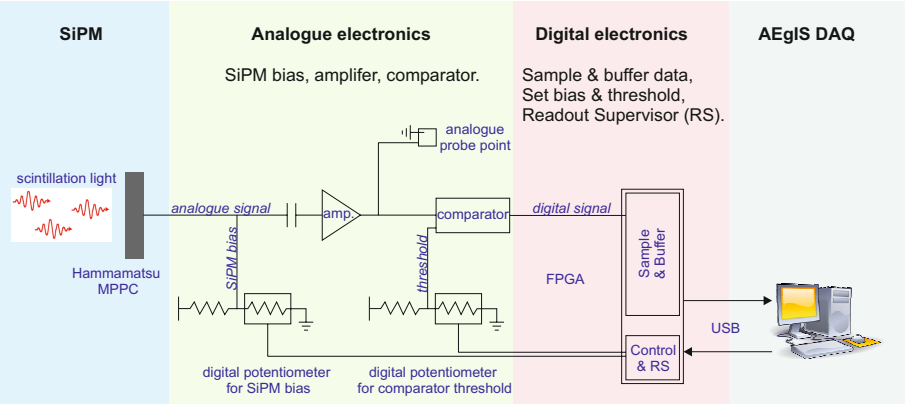

Figure 7. Readout architecture for the FACT detector. The analogue electronics consists of custom PCBs and the digital electronics makes use of off-the-shelf FPGA evaluation boards.

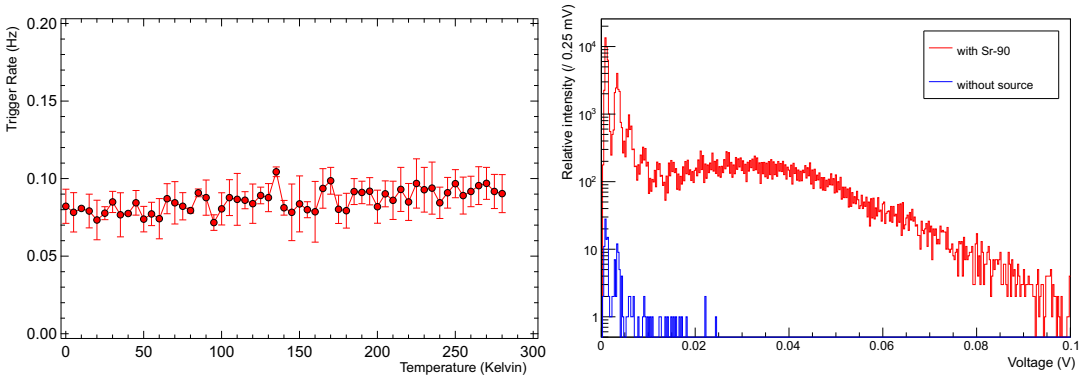

Figure 8. *Left*: temperature dependence of cosmic trigger rate in scintillating fiber. *Right*: photoelectron spectra of a FACT scintillating fiber on the top row of the outer layer exposed to a Sr-90 beta source. The fibers immediately beneath this fiber on the bottom row are used to form the trigger. The first four photoelectron peaks correspond to dark counts, which are recorded when the electron passes through one of the bottom row fibers without passing through the top row fiber.

The MPPC signal is connected to a fixed gain linear amplifier which produces a pulse with an amplitude of 10 mV for each photoelectron and a duration of 10 ns. The amplified signal is connected to a fast discriminator with a TTL output that can be read directly by an FPGA. A dual channel potentiometer is used to adjust the comparator threshold and bias voltage for each MPPC channel. The TTL output of 48 comparators is connected to a Xilinx Spartan-6 SP605 FPGA, which samples the output at 200MHz for the duration of the antihydrogen production period. The FPGA is also used to program the registers of the dual channel potentiometers. A schematic of the readout architecture is shown in 7.

4 Results

4.1 Tests of scintillating fibers at cryogenic temperatures with cosmic rays

Tests have been performed to study the light yield and lifetime of scintillating fibers at cryogenic temperatures. The setup consists of 3 layers of 1 mm diameter Kuraray scintillating fibers ar-

ranged in loops at the bottom of a liquid helium cryostat. The light from each of the scintillating fibers is detected by 3 Hamamatsu MPPCs (S10362-11-100C), the output of which is amplified and digitized by a LeCroy Wavepro 7100 10 GS/s oscilloscope. The scintillating performance is measured by the response of the scintillating fibers to the passage of cosmic rays. The oscilloscope is triggered whenever the signal of two of the three fibers exceeds 4 photoelectrons and an event is defined when a signal is observed in the third fiber, corresponding to the passage of a cosmic ray through all 3 scintillating fiber layers. The cryostat is completely filled with liquid helium which immerses the fibers for 4 hours. The rate of events is measured during the cool down, at 4 K and during the warm up back to ambient temperature. The rate of events as a function of temperature is shown in figure 8 and reveals no meaningful decrease in the light yield of the scintillating fibers at cryogenic temperatures. Examination of the fibers under a microscope after a number of thermal cycles to 4 K does not reveal any sign of mechanical damage to the fibers.

4.2 Tests of the FACT detector with a Sr-90 beta source

Before insertion into the AEgIS apparatus the assembled FACT detector and readout electronics were tested with a collimated 2.5 MBq Sr-90 beta source (0.546 MeV, 2.28 MeV). The source was directed at a fiber on the top row of the outer layer and a trigger formed from the amplified analogue output of the MPPCs connected to the fibers immediately beneath the target fiber on the bottom row of the outer layer. The resulting photoelectron spectra of the target fiber is shown in figure 8. It is geometrically possible for the electrons to pass through one of the bottom row fibers without passing through the top row fiber and this leads to the dominant first four photoelectron peaks. However, a clear signal from the beta source is evident, which provides confidence that the light transmission chain for the target fiber is reasonable.

4.3 UV light injector

It is impractical to test all fiber channels with the Sr-90 source since it is very time consuming and the electrons are absorbed before reaching the fibers of the inner layer. Furthermore, tests with a radioactive source are impractical once the FACT detector is installed inside AEgIS. However, it is important to be able to monitor the performance of the scintillating fibers and the light transmission chain once the detector is installed. Consequently a method has been developed for FACT that uses UV light to stimulate the scintillating fibers. The systems consists of a Thorlabs 700 mA 365 nm UV LED the light of which is injected into two clear quartz fibers which are fixed along the length of the inner and outer layers of the scintillating fiber tracker. Ultra fine sandpaper is used to remove the outer cladding along the length of the fiber that is directly above the scintillating fibers. The power of the LED is adjusted to reproduce the spectra obtained with the Sr-90 source. The system has been implemented and used to verify the operation of the scintillating fibers at cryogenic temperatures.

5 Conclusion

The detection of antihydrogen production is a crucial requirement for the AEgIS experiment. A scintillating fiber tracker with silicon photomultiplier readout has been developed to operate at cryogenic temperatures. A readout system has been developed that provides bias and comparator

threshold control for each channel and uses off-the-shelf FPGA evaluation boards for the digital electronics. The detector has been installed in the AEgIS apparatus and tested with a UV light injection system. Commissioning with antiprotons will take place during the autumn 2014 antiproton run at CERN.

Acknowledgments

We wish to acknowledge the technical contributions of R.Hanni, P.Lutz, J.Rochet, C.Tognina and J.M.Vuilleumier. This work was supported by: Swiss National Science Foundation grant no. 142436, European Research Council grant no. 291242-HBAR-HFS and the Austrian Ministry for Science and Research, DFG research grant, Excellence initiative of Heidelberg University, Research Council of Norway, Bergen Research Foundation, Istituto Nazionale di Fisica Nucleare (INFN- Italy).

References

[1] M. Doser et al., *Exploring the WEP with a pulsed cold beam of antihydrogen*, *Class. Quantum Grav.* **29** (2012) 184009.

[2] A. Kellerbauer et al., *Proposed antimatter gravity measurement with an antihydrogen beam*, *Nucl. Instrum. Meth.* **B 266** (2008) 351.

[3] S. Aghion et al., *A moiré deflectometer for antimatter*, *Nat. Commun.* **5** (2014) 4538.

[4] S. Aghion et al., *Prospects for measuring the gravitational free-fall of antihydrogen with emulsion detectors* , 2013 *JINST* **8** P08013.

[5] S. Aghion et al., *Detection of low energy antiproton annihilations in a segmented silicon detector*, 2014 *JINST* **9** P06020.

[6] M. Kimura et al., *Development of nuclear emulsions with 1 µm spatial resolution for the AEgIS experiment*, *Nucl. Instrum Meth.* **A 732** (2013) 325.

[7] M. Amoretti et al., *Production and detection of cold antihydrogen atoms*, *Nature* **419** (2002) 456.

[8] G.B. Andresen et al., *Trapped antihydrogen*, *Nature* **468** (2010) 673.

[9] Kuraray, www.kuraray.co.jp/en.

[10] Hamamatsu Photonics, www.hamamatsu.com.

[11] H. Kawamuko et al., *Fiber connector for MPPC*, PoS(PD07)043.